

## ARTICLE OPEN



# The evolution of social-ecological system interactions and their impact on the urban thermal environment

Bin Chen<sup>1</sup>, Fanhua Kong<sup>1</sup>, Michael E. Meadows<sup>1,2</sup>, Huijun Pan<sup>1</sup>, A-Xing Zhu<sup>3,4</sup>, Liding Chen<sup>5</sup>, Haiwei Yin<sup>6</sup> and Lin Yang<sup>1</sup>

While heat mitigation is crucial to achieving sustainable urban development, an inadequate understanding of the evolution of the urban thermal environment (UTE) and its relationship with socio-ecological systems (SESs) constrains the development of effective mitigation strategies. In this study, we use satellite observations from 2000–2021 to explore the evolving impact of SES interactions on the UTE of 136 Chinese urban areas. The results reveal a nonlinear intensification of the UTE over the period and an indication that an increasing number of urban areas have successfully applied UTE mitigation measures. Spatio-temporal patterns in UTE are shown to be strongly influenced by social and ecological factors and their interactions, whereby the higher the SES status, the stronger the decreasing UTE trend. These findings highlight the need for, and advantages of, developing win-win solutions for urban society and ecology and have important implications in creating integrated strategies for heat mitigation in promoting urban sustainability.

npj Urban Sustainability (2024)4:3; <https://doi.org/10.1038/s42949-024-00141-4>

## INTRODUCTION

The Anthropocene world is increasingly urbanizing, and the intensity of the urban heat island effect, whereby urban temperatures are higher relative to the surrounding rural areas<sup>1</sup>, is escalating in most cities<sup>2</sup>. Meanwhile, driven by global climate change, the magnitude, frequency and duration of heat waves in cities are all on the increase<sup>3</sup>. Deterioration of the urban thermal environment (UTE) threatens human health, exacerbates both energy consumption and air pollution<sup>4,5</sup> and has become a critical challenge to habitable cities and sustainable urban development. However, the UTE is complex and affected by interactions between a range of factors<sup>6,7</sup>. As urbanization progresses, nature is transformed and increasingly coupled with society, forming a social-ecological system (SES) characterized by changes in surface structure and energy flow that directly affect the UTE. Currently, evolution of the UTE is poorly understood and, if more holistic and effective mitigation strategies are to be developed and applied, it is important to explore how the urban SES has developed over time and its impacts on the UTE<sup>8,9</sup>.

Understanding the spatial and temporal characteristics of the UTE, an important starting point for heat mitigation, is facilitated by remote sensing technology, which has the characteristics of availability, global coverage and high spatial resolution. Land surface temperature and surface urban heat island intensity are common representations of UTE<sup>2,6</sup>. The surface UTE exhibits spatial (from local to global) and temporal (diurnal, seasonal, and interannual) variation, although there is general consensus that the global mean surface urban heat island intensity is greater during the day than at night<sup>10,11</sup>, and that land surface temperature anomalies are greatest during summer<sup>12</sup>. In contrast, interannual variation patterns, important in systematically understanding the evolution of the UTE, are not yet fully resolved<sup>13,14</sup> and marked spatial heterogeneity is evident. For example, the

surface urban heat island enhancement trend is greater in the rapidly urbanizing parts of Asia and Africa than in the more stable urbanizing or highly urbanized regions of Europe and North America<sup>15,16</sup>, indicating that UTE trends may vary at different stages of urban development. Therefore, a key question remains as to whether there are multiple steady states of the UTE during urban development. Moreover, whether the relationship between the stages of urban development and surface urban heat island may be consistent with the Environmental Kuznets Curve, thereby implying that UTE evolution follows an inverted *U*-curve pathway<sup>17,18</sup>, this pattern requires further validation against multiple samples over a longer time series.

Fundamentally, the UTE changes in response to variations in a range of influencing factors and spatial analysis suggests that it is influenced both by social subsystems (e.g., population density, area of impervious surface) and by ecological subsystems (e.g., blue and green spaces)<sup>7,12,19</sup>. In the absence of time-series data, analyses based on the substitution of space for time provide valuable insights into the dynamics of the UTE<sup>17</sup>. However, in the process of urban development, the structure, function and critical feedbacks of a complex SES undergo dynamic changes and, due to the paucity of appropriate time series data, only a few studies have focused on the role of a particular social or ecological factor on the UTE<sup>15,20</sup>. In addition, because advancing heat mitigation strategies from the SES perspective in an integrated manner requires identifying critical feedback pathways<sup>21</sup>, it is necessary to measure and account for the evolving impact of interactions between social and ecological factors with the UTE using a systemic approach.

As a complex system, the SES connects social and ecological subsystems through feedback pathways comprising interactions between the contributing factors (Fig. 1)<sup>21,22</sup>. The complex structure of SESs generates dynamic processes in a continuously evolving manner, especially so during rapid urbanization<sup>23</sup>.

<sup>1</sup>School of Geography and Ocean Science, Nanjing University, Xianlin Ave.163, 210023 Nanjing, China. <sup>2</sup>Department of Environmental & Geographical Science, University of Cape Town, Rondebosch 7701, South Africa. <sup>3</sup>Department of Geography, University of Wisconsin-Madison, Madison, WI, USA. <sup>4</sup>Key Laboratory of Virtual Geographic Environment (Nanjing Normal University), Ministry of Education, Nanjing 210023, China. <sup>5</sup>School of Ecology and Environmental Science, Yunnan University, 650091 Kunming, China. <sup>6</sup>School of Architecture and Urban Planning, Nanjing University, No. 22, Hankou Road, 210093 Nanjing, China. <sup>✉</sup>email: fanhuakong@nju.edu.cn; fanhuakong@163.com; michael.meadows@uct.ac.za

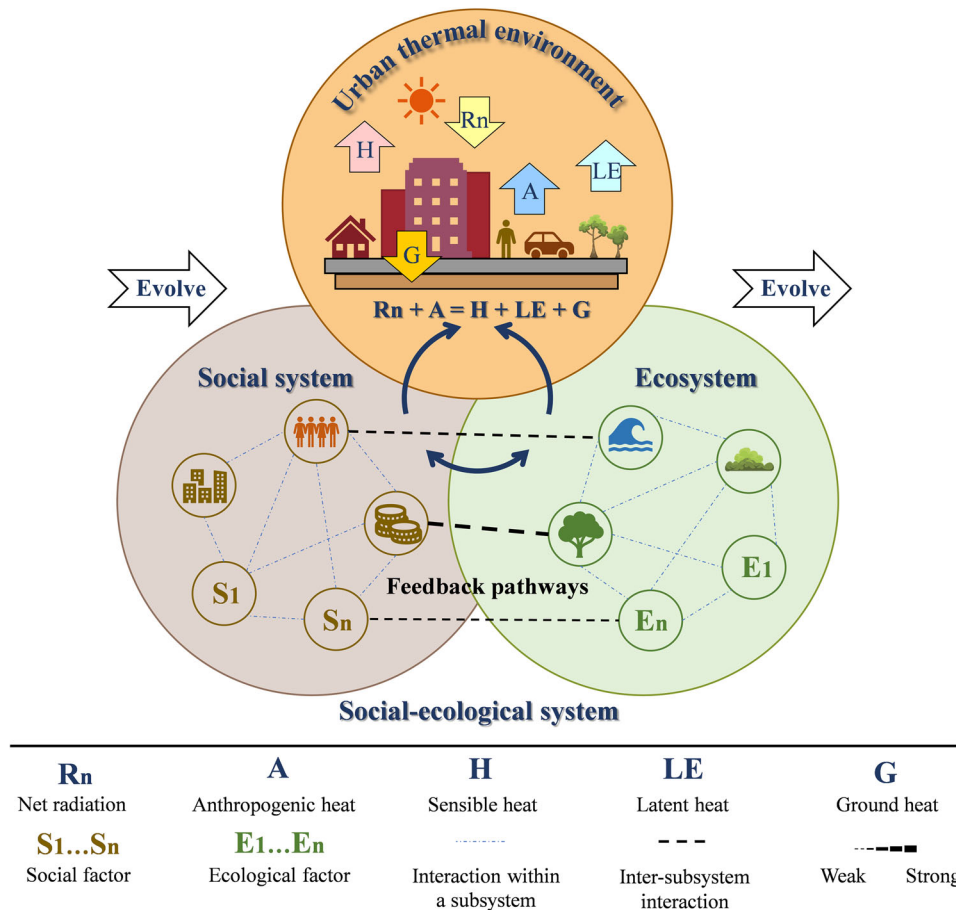


**Fig. 1 Conceptual framework for exploring the impact of social-ecological system interactions on the urban thermal environment.** Orange circles represent energy flow processes in urban areas, coffee-colored circles represent social system and green circles represent ecosystem. Blue dotted lines indicate interactions between factors within a subsystem; black dotted lines indicate interactions between social and ecological factors (inter-subsystem interaction).

Although SES concepts have shown potential in addressing seemingly intractable social and environmental challenges, much previous work has been theoretical rather than practical<sup>22</sup>. Given the urgent need to counter the ongoing deterioration of UTE, a conceptual framework is proposed to understand the nature, and degree of impact, of the SES on the UTE (Fig. 1). Factors, including numerous social and ecological factors, are the basic components of the SES structure. Variations in directly or indirectly alter the surface energy balance, consequently affecting the UTE. Furthermore, these factors not only collectively impact UTE, but they also exhibit intricate interdependence. Feedback pathways reveal the interaction between social and ecological factors from an SES perspective. For instance, urban expansion fosters population growth and encroachment of impervious areas into ecological land, resulting in increased anthropogenic heat and surface heat absorption and storage, thereby exacerbating UTE degradation. In contrast, increasing ecological land in densely populated areas through the construction of urban green corridors restricts the absorption of energy by the surface from industrial areas, residential centers, etc., contributing to the alleviation of urban heat. Ultimately, the integration of multiple feedback pathways serves to characterize SES and thus unveil the relationship between the SES and UTE (Fig. 1).

Based on this conceptual framework, we conducted practical research that addresses the challenge of developing holistic strategies for urban heat mitigation. In the process, we evaluated the thermal environment status of 136 urban areas of large cities (urban population over one million) in China over the period

2000–2021 using the difference in land surface temperature between urban areas and surrounding reference areas, with a view to understanding the spatio-temporal characteristics of UTE development. In exploring the underlying mechanisms of the evolving UTE from the SES perspective, we first quantified the role of social factors, ecological factors and social and ecological interactions on the UTE. Thereafter, to examine the response of the UTE to SES dynamics, we constructed a social-ecological state index (SESI), which is oriented to the UTE through multiple SES feedback pathways. Thresholds in the impact of the SES on the UTE are identified for revealing the importance of achieving win-win solutions in the synergistic development of society and ecological systems for heat mitigation.

## RESULTS

### Evolutionary characteristics of the urban thermal environment

Overall, urban temperatures are higher than the surrounding area, and there is clear evidence of a distinct UTE in all 136 urban areas over the past 22 years, with an average  $\Delta T$  of  $+2.83$  °C between 2000–2021 (Supplementary Table 1). The magnitude of change in UTE intensity is spatially heterogeneous (Fig. 2). Cities located in the southeast exhibit a relatively high magnitude of change in  $\Delta T$ . In contrast, cities in central China have a relatively low magnitude of change in  $\Delta T$ . Furthermore, as indicated in the scatter plot in Fig. 2, the mean thermal environment of the 136 urban areas exhibits an accelerating trend. For example, 124 (91.18%) of the

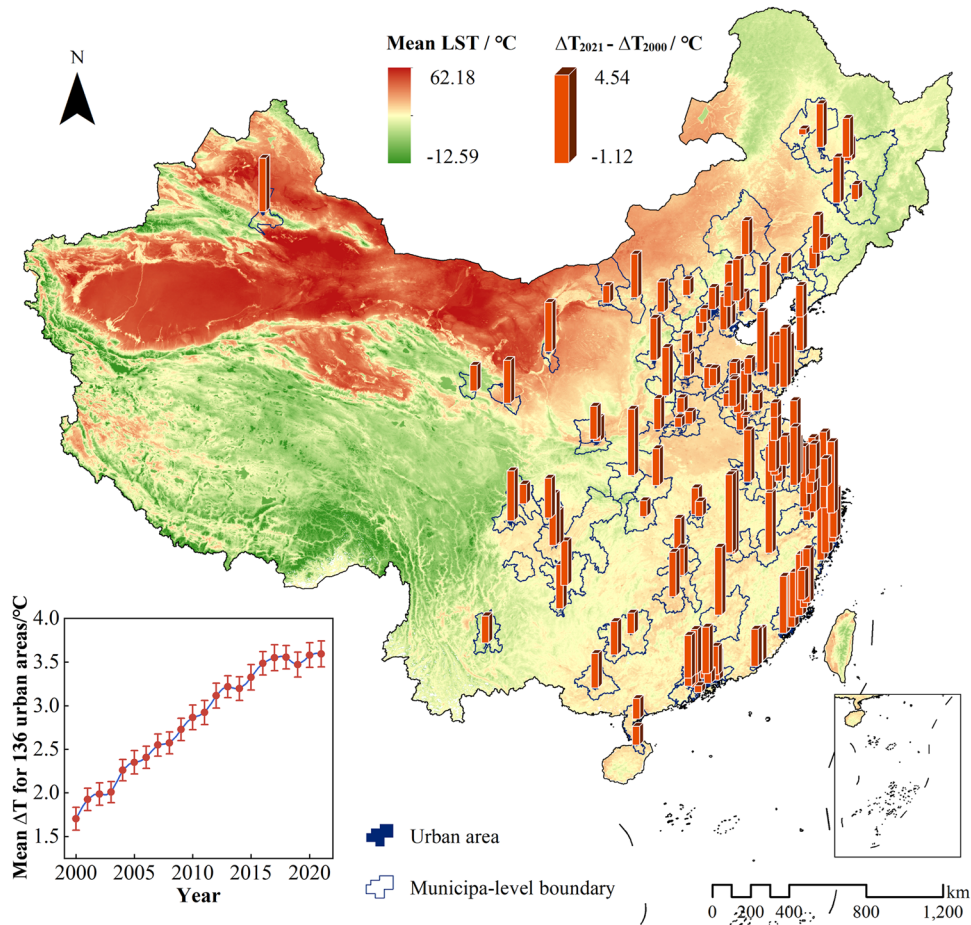


**Fig. 2** The changes in summer daytime  $\Delta T$  in each urban area from 2000 to 2021. The background information depicted in the figure represents the 22-year mean summer daytime land surface temperature in China, which has been calculated using the MOD11A2 land surface temperature datasets. The scatterplot presents the interannual variability of the average thermal environment in 136 urban areas. Error bars refer to  $\pm 1$  standard deviation.

urban areas, present a significantly increasing  $\Delta T$  trend over time (two-tailed  $t$  test,  $p < 0.05$ ) with an annual average positive trend of  $0.10 \pm 0.04$  (mean  $\pm$  standard deviation) (Supplementary Fig. 1).

Inflection points in the  $\Delta T$  records, whereby there is a marked deviation in the trend line that indicates a shift in the intensity or direction of temperature difference at a particular time, are evident in a substantial proportion (42; 30.88%) of the urban areas (Fig. 3a). In general, the presence of inflection points reveals nonlinearity in the temporal trend of UTE intensity, and three of the urban areas even exhibit two clear inflection points, i.e., three distinct phases of temperature change (Supplementary Fig. 1). A greater proportion of cities (38) have trends in  $\Delta T$  that shifted during the last two decades from increase to decrease than those where  $\Delta T$  trends changed from decrease to increase (7) (Fig. 3b). Moreover, we observe a higher frequency of  $\Delta T$  inflection points that shift to slower rates of increase during the last two decades. In contrast, slower to faster warming inflection points occur mainly in the early phase of the time series. The trend in  $\Delta T$  inflection points from faster to slower warming indicates that the UTE is being mitigated in an increasing number of urban areas.

Spatial analysis further indicates that heat mitigation is not restricted to the local scale, and that inflection points in  $\Delta T$  trends occur widely across the country. Notably, a relatively large number of urban areas with decreasing  $\Delta T$  trends are located in regions of China that are the most highly urbanized and have the fastest growing economies<sup>24</sup>, including the Beijing-Tianjin-Hebei urban

agglomeration, the Yangtze River Delta urban agglomeration and the Pearl River Delta urban agglomeration (Fig. 3a).

Figure 3 and Supplementary Fig. 1 indicate that, while the vast majority of urban areas ( $n = 82$ ) are associated with an overall rate of  $\Delta T$  increase over time (Fig. 3c), many exhibit more irregular rates of change. In a number of cases, inflection points in the trend lines suggest that there may be distinct phases of change over the last 22 years. For example, some urban areas exhibit an initial decline in  $\Delta T$ , followed by a steep increase (Fig. 3d), or have a relatively slow rate of increase followed by an acceleration (Fig. 3e), while others are observed to change from relatively rapid rates of temperature increase to a lower rate (Fig. 3f) or even to a negative trend (Fig. 3g). Moreover, some urban areas ( $n = 12$ ) show a completely irregular change of  $\Delta T$ , so these are excluded from the subsequent analysis. Based on the observed patterns of change over time, three phases in the UTE trends can be identified (Supplementary Fig. 2). There are 77 occurrences where slope values lie above the average rate of  $\Delta T$  increase (0.1), i.e., rapid increase phase, 76 where the slope =  $< 0.1$  but  $> 0$ , i.e., slow increase phase; and a further 28 that are characterized by slope =  $< 0$ , and accordingly classified as decrease phase.

### The impact of social-ecological system interactions on the urban thermal environment

Typically, social factors may be expected to have a reinforcing effect on UTE increase, while ecological factors would have a

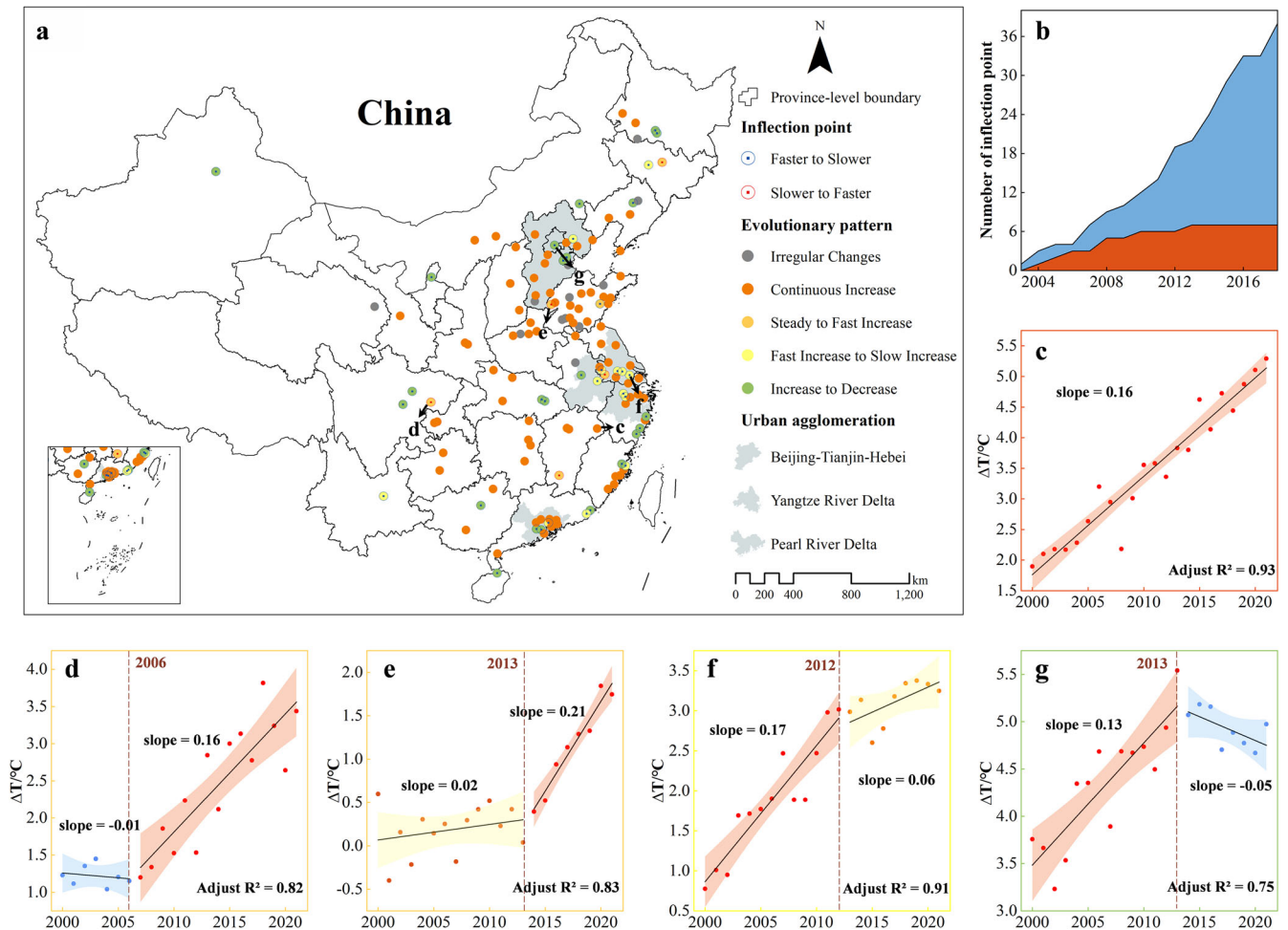


**Fig. 3** Trends in urban thermal environment, 2000 to 2021, showing inflection points where the rate or direction of trend changes. **a** Each circle represents one of the 136 urban areas, different colours represent various evolutionary patterns. The gray background represents the urban agglomerations (identified based on municipal-level administrative boundaries). **b** The cumulative number of inflection points over time. Blue and red shading represent negative and positive trend in  $\Delta T$ , respectively. **c** Trend of  $\Delta T$  in Shangrao urban area, consistent increase, i.e., no inflection point. **d** Trend of  $\Delta T$  in Nanchong:  $\Delta T$  inflection point shifts from negative to positive. **e** Trend of  $\Delta T$  for Liaocheng:  $\Delta T$  inflection point shifts from steady increase to faster rate of increase. **f** Trend of  $\Delta T$  in Suzhou:  $\Delta T$  inflection point shifts from faster to slower rate of increase. **g** Trend of  $\Delta T$  in Beijing:  $\Delta T$  inflection point from increase to decrease. The shaded area around the fitted line represents the 95% confidence interval.

mitigating impact. Indeed, statistical relationships among the basic components in SESs (Fig. 1) do reveal a significant positive correlation between  $\Delta T$  and social factors, including population density,  $NL_{VA}$  and impervious area percentage, while  $\Delta T$  exhibits a significant negative correlation with ecological factors, including ecological land percentage and  $\Delta EVI$  (two-tailed  $t$  test,  $p < 0.01$ ) (Supplementary Fig. 3). Moreover, social and ecological factors are significantly negatively correlated (two-tailed  $t$  test,  $p < 0.01$ ), indicating the occurrence of trade-offs between social and ecological factors in the urban development process.

We compared the trends in social and ecological factors during the various thermal environmental phases (Fig. 4b). In the rapid increase phase of the UTE, social factors increase dramatically, with the trends in economic growth and urban expansion (mean  $NL_{VA}$  slope = 0.02, mean impervious area percentage slope = 1.52) are stronger than those of the slow increase and decrease phases. Meanwhile, ecological factors exhibit a sharp decline trend (mean  $\Delta EVI$  and ecological land percentage slope:  $-0.006$  and  $-1.52$ , respectively) during the rapid increase phase. In the slow increase phase of the UTE, the increasing trends of social factors are weaker than those in the rapid increase phase. The ecological factors exhibit a weaker declining trend compared to the rapid increase

phase, with mean  $\Delta EVI$  and ecological land percentage slopes of  $-0.003$  and  $-1.15$ , respectively. In the decreasing phase of the UTE, social factors still primarily show an upward trend. The degradation trend of ecological factors (mean  $\Delta EVI$  slope =  $-0.001$ , mean ecological land percentage slope:  $-0.77$ ) is weaker than in the rapid and slow increase phases, and in some urban areas,  $\Delta EVI$  shows an upward trend.

Factor analysis using geographical detector reveals economic development to be the key social factor underlying the various UTE phases ( $q(NL_{VA}) = 0.560$ , two-tailed  $t$  test,  $p < 0.01$ ), while vegetation quality is the dominant ecological factor ( $q(\Delta EVI) = 0.442$ , two-tailed  $t$  test,  $p < 0.01$ ) (Fig. 4a). In addition, the percentage of impervious area and percentage of ecological land, factors that represent quantitative characteristics of social and ecological system, are shown by their respective  $q$ -values (0.368 and 0.366; two-tailed  $t$  test,  $p < 0.01$ ) to have also exerted a strong influence on the UTE. Indeed, the percentages of impervious area and ecological land are evidently inversely proportional to each other. The maximum mean slope (1.52) of the impervious area percentage occurred during the rapid increase phase of the UTE, while the minimum (0.75) occupied the decreasing phase (Fig. 4b). Correspondingly, the average slope of the percentage of

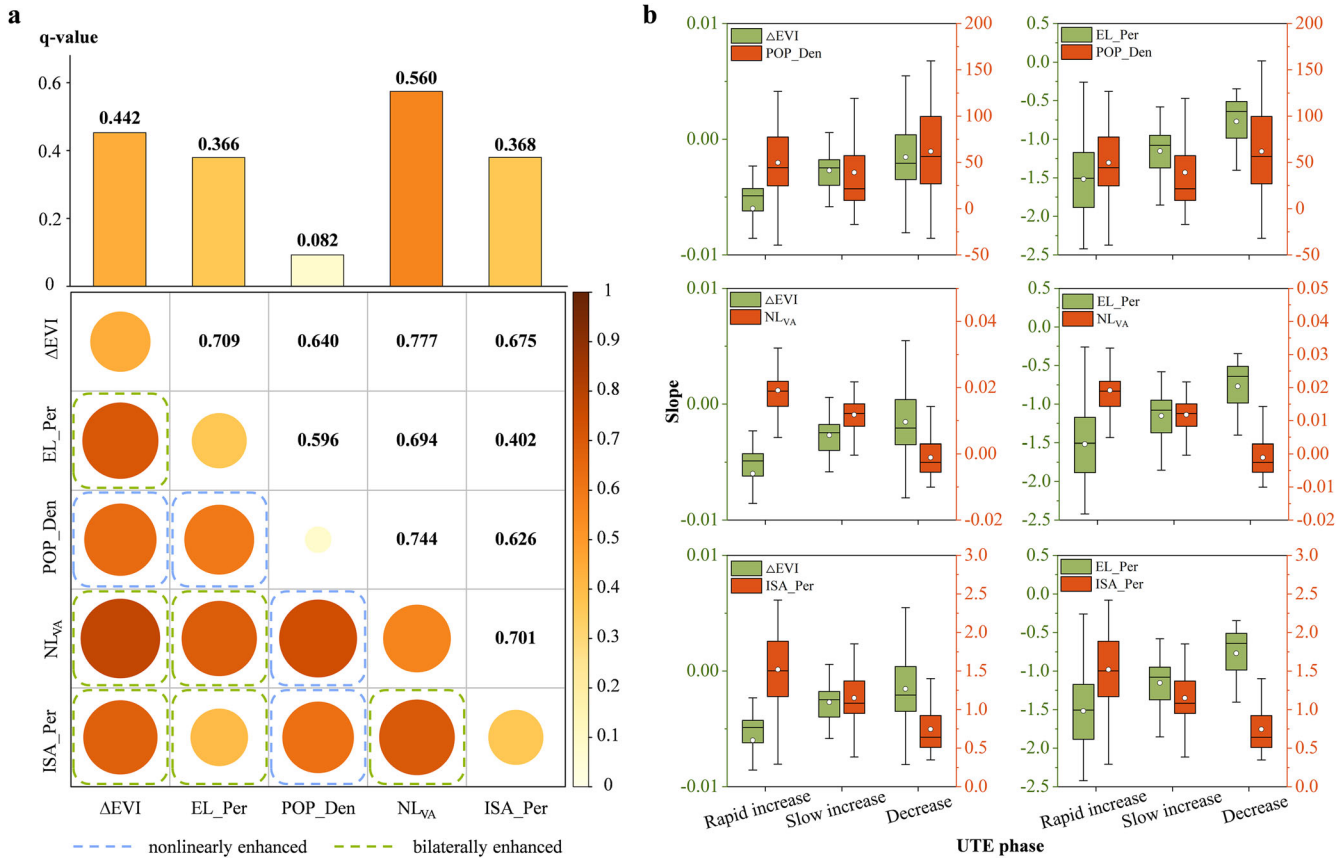


**Fig. 4** Effects of social and ecological factors on the urban thermal environment. **a** Effects of single social or ecological factors and the interaction effects for each pair of factors on the UTE phases. Circles without dashed boxes and bar graph represent single factor effects, while circles with dashed boxes represent paired factor effects. Light to dark colors represent q-values from low to high. **b** Trends in the paired social and ecological factors across the UTE phases. Box plots show the interquartile range (IQR) (box), the median (horizontal line in box), the mean (hollow circle in box),  $1.5 \times$  IQR (whiskers) and maximum/minimum (horizontal lines outside box).

ecological land was  $-1.52$ ,  $-1.15$  and  $-0.77$  during the rapid increase, slow increase, and decrease phases, respectively. Accordingly, the data here indicate that economic development and vegetation quality are the most important social and ecological factors influencing the UTE in China over the last two decades.

We further explored the contribution of the interaction of social and ecological factors on the various UTE phases. Figure 4a illustrates that population density exhibited nonlinearly enhanced interactions with other factors, i.e., the q-value of two factors is greater than the sum of the q-values of the individual factors. Interaction between population density and  $\Delta$ EVI and ecological land percentage contributed 0.640 and 0.596 to the UTE phases, respectively. Both NL<sub>VA</sub> and impervious area percentage exhibit bivariate enhanced interactions with ecological land percentage and  $\Delta$ EVI, meaning that the q-value of two factors is higher than the q-value of a single factor and lower than the sum of the q-values of the individual factors. The strongest interaction effect is between NL<sub>VA</sub> and  $\Delta$ EVI ( $q(\text{NL}_{VA} \cap \Delta\text{EVI}) = 0.777$ ). Taken together, in demonstrating that the interaction of social and ecological factors may have enhanced effects on UTE, the study provides a clear indication that urban heat mitigation strategies need to evolve from a single factor approach to consider multiple factor interactions.

The SESI exhibits significant differences across the UTE phases (one way ANOVA,  $F = 76.830$ ,  $p < 0.01$ ). The decrease phase has the highest SESI mean value (0.496), and the rapid increase phase exhibits the lowest value (0.035) (Fig. 5a). The distribution curves in all three phases indicate the occurrence of a single peak, across

the different SESI values (Fig. 5a). The interquartile range of the SESI index ranges from low to high across the rapid increase phase ( $-0.117$  to  $0.192$ ), slow increase phase ( $0.170$  to  $0.395$ ), and decrease phase ( $0.412$  to  $0.586$ ). It is clear from these results that SES status assists in alleviating the UTE and that higher SESI values are associated with enhanced UTE mitigation effects.

We further explored the relationship between the computed SESI and  $\Delta T$  trends through piecewise linear regression. Figure 5b reveals the occurrence of a marked change in the UTE effect of increasing SESI. At SESI values below the inflection point (0.414), for every 0.1 increase in SESI, the  $\Delta T$  slope decreases by approximately 0.025, whereas at values above the inflection point, the effect is larger by 0.095 for every 0.1 increase. This suggests that there is a threshold of SESs impact on the thermal environment. When the SES develops beyond a certain stage, the thermal environment becomes more rapidly mitigated.

Our spatial analysis reveals the recent state of SESs in each urban area (Fig. 5c). Recent SESI values have significant differences between urban areas. Specifically, the three highest SESI values are located in Fuzhou (0.701), Wuhan (0.636) and Urumqi (0.609), respectively, while the three lowest SESI values are located in Nanchang ( $-0.197$ ), Ganzhou ( $-0.195$ ) and Suzhou ( $-0.160$ ), respectively (Supplementary Table 2). We also observed spatial heterogeneity in the distribution of recent SESI. As shown in Fig. 5c, the urban area in northeast China has a relatively positive SES status oriented to the UTE, with an average SESI value of 0.467. The urban area in southwest China has a relatively low average SESI value of 0.189, suggesting that SES development in these cities is likely to accelerate urban warming and exposure to

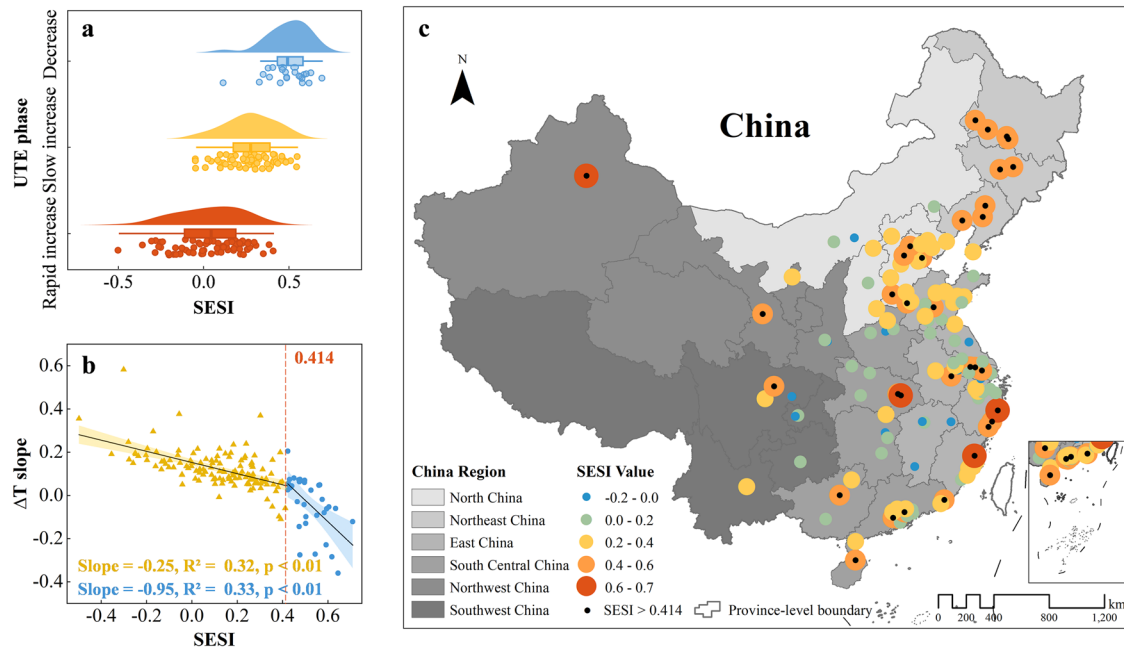


**Fig. 5** Response of urban thermal environment to the social-ecological system. **a** Distribution of social-ecological status index (SESI) across the three UTE phases. Box plots show the interquartile range (IQR) (box), the median (vertical line in box) and  $1.5 \times \text{IQR}$  (whiskers). **b** Relationship between UTE trends and SESI. The shaded area around the fitted line represents the 95% confidence interval. A two-tailed  $t$  test was used to examine the statistically significant level ( $p$ -value). **c** Spatial distribution of recent SESI values in each urban area. Different shades of gray background represent distinct geographical regions (identified based on province-level administrative boundaries).

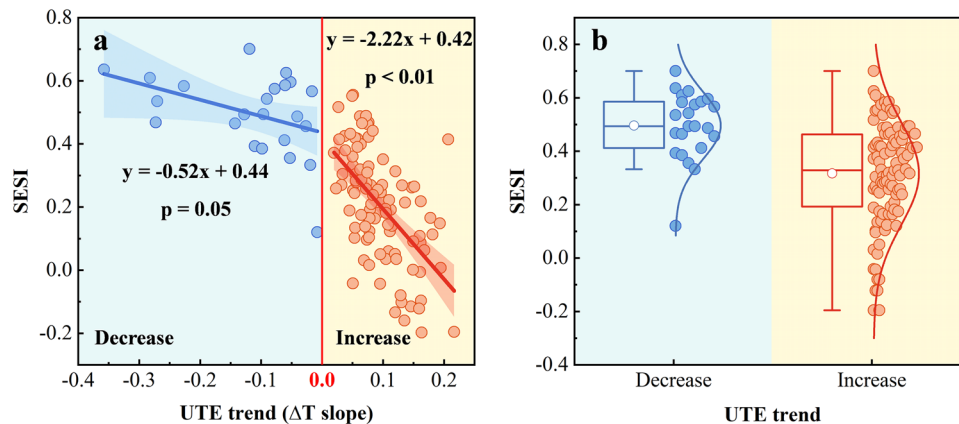


**Fig. 6** Differences in recent social-ecological system status in different urban thermal environment trends. **a** Relationship between  $\Delta T$  slope and SESI in different UTE trends. The shaded area around the fitted line represents the 95% confidence interval. A two-tailed  $t$  test was used to examine the statistically significant level ( $p$ -value). **b** Distribution of SESI in different UTE trends. Box plots show the interquartile range (IQR) (box), the median (horizontal line in box), the mean (hollow circle in box),  $1.5 \times \text{IQR}$  (whiskers) and maximum/minimum (horizontal lines outside box).

higher heat stress. Furthermore, the SESI is greater than the threshold ( $\text{SESI} = 0.414$ ) in 31 of the urban areas, most of which are located in eastern China, indicating that SES development has contributed to UTE mitigation in these cities. More urban areas ( $n = 93$ ) still have SESI values below the threshold and are priority areas for future heat mitigation.

#### Differences in social-ecological system status at different urban thermal environment trends

At present, the thermal environment in 23 urban areas is experiencing a decreasing trend, while 101 urban areas are witnessing an increasing trend. Regardless of whether the urban areas with an increasing or decreasing trend in the UTE, there is a positive correlation between thermal environment reduction and

SESI increase (Fig. 6a). SESI values are more sensitive to changes in UTE when UTE is on a decreasing trend, implying varying development patterns for SESs in different UTE trends. Comparatively, the average SESI value for urban areas with a decreasing trend in the UTE is 0.496, which is higher than in urban areas with an increasing trend (mean SESI value = 0.316) (Fig. 6b). This indicates that a high SESI value signifies a SES state that helps alleviate the UTE. Further analysis indicates that, compared to urban areas with an increasing trend in the UTE, the urban areas with a decreasing trend have effectively restrained the degradation trend of ecosystems, and slowed down the trend of urban expansion (The mean slopes of  $\Delta \text{EVI}$ , ecological land percentage and impervious area percentage in the UTE decreasing trend are  $-0.001$ ,  $-0.77$ , and  $0.75$ , respectively; the mean slopes in increasing trend are  $-0.003$ ,  $-1.27$ , and  $1.27$ ) (Supplementary

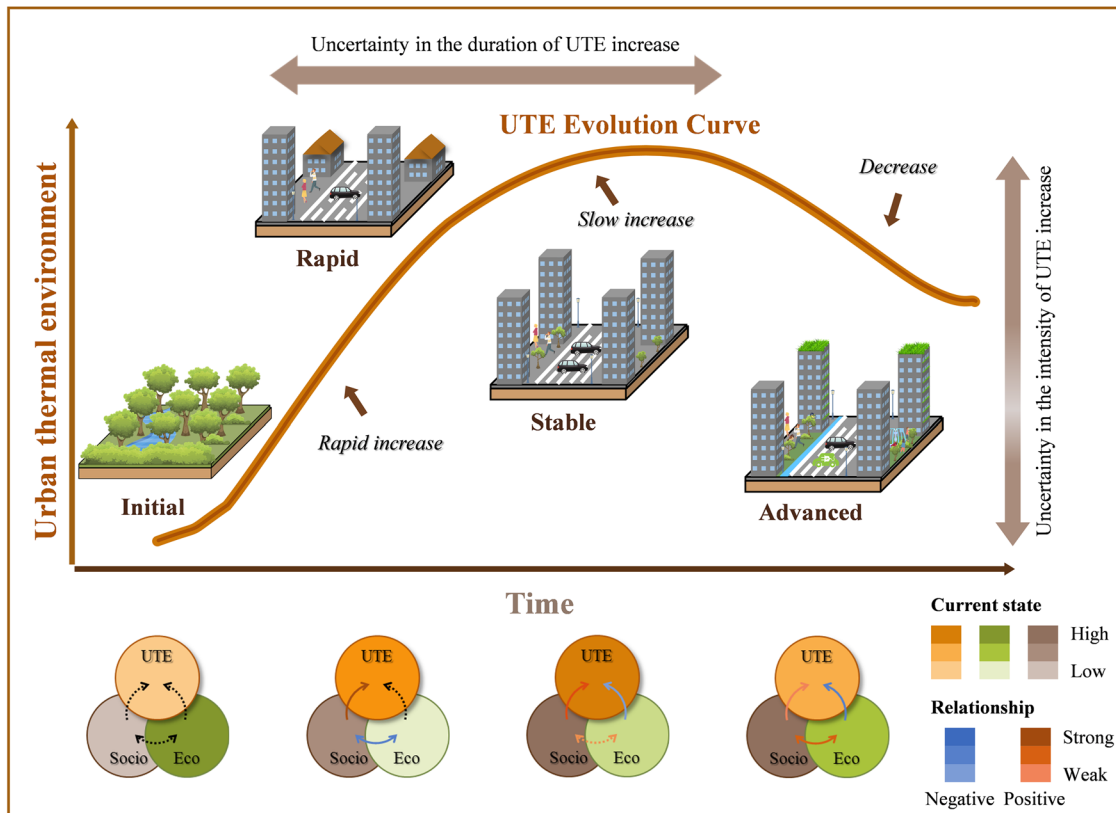


**Fig. 7 Conceptual model of the evolving relationship between social systems, ecosystems and the urban thermal environment during the urban development process.** Light to dark shading in each colour represents low to high values respectively. Arrows represent the nature of the relationship between two components as follows: grey = no relationship, blue = negative correlation, orange = positive correlation, light to dark colours represent low to high correlation coefficients respectively; solid lines represent statistically significant correlations, dashed lines represent no statistical significance.

Fig. 4). In particular, we observed an increasing trend in  $\Delta EVI$  in urban areas such as Beijing, Fuzhou and Yinchuan.

## DISCUSSION

The ability to manage complex SESs determines the success or failure of ecological and socioeconomic sustainability policies<sup>9</sup>. This study reveals nonlinear trends of temperature increase in the UTE, and highlights the dynamic link between the SES and UTE. The results offer support for the application of SES theory to policymaking, and provide an integrated perspective in addressing the diverse negative impacts of warming urban climates.

In contrast to the commonly recorded situation whereby the intensity of the UTE continues to increase over time<sup>15,16</sup>, we observed the occurrence of decreasing UTE intensity and that this appears to be increasing over time. This may in part be attributed to the implementation of policies and measures focused on eco-environmental protection in China, such as “eco-city”, “low-carbon city” and “sponge city”, and an increasing focus on urban greening and nature-based solutions<sup>25,26</sup>. Nature-based solutions offer multiple benefits to cities and address diverse social challenges, including reducing disaster risk, enhancing climate resilience, restoring biodiversity, and providing opportunities for recreation that has beneficial health effects<sup>27–29</sup>. Urban parks are not only cooling islands, but by juxtaposing several parks it is possible to construct ecological corridors and further prevent expansion of the UTE<sup>30</sup>. Furthermore, urban forests reduce UTE by shading building surfaces, deflecting solar radiation and releasing moisture into the atmosphere<sup>31</sup>. Of course, urban development is not simply a two-dimensional phenomenon, but has also been characterized by vertical expansion which may be an additional

mitigating factor. Urban development initially involves the rapid encroachment of impervious surfaces on ecological land but escalation of urban land prices often results in a shift to high-rise buildings that may reduce daytime surface temperatures by blocking a proportion of solar radiation in large shaded areas<sup>32,33</sup>. In summary, despite continued global warming, a range of adaptation and mitigation measures have the potential to curb the rapid growth of UTE<sup>34,35</sup>.

The study reveals the occurrence of three phases in the evolving UTE over the last two decades, viz. a rapid increase phase, slow increase phase, and a decreasing phase, and that these exhibit a clear relationship to SESs dynamics. These phase shifts may be related to goal-directed decisions and actions by urban administrations as urban development unfolds. Based on our multi-city sample analysis, the relationship between urban development and the evolving UTE conforms to the Environmental Kuznets Curve (Fig. 7). We have further characterized the characteristics of UTE and the SES in different urban development periods. Originally, urban areas have more natural surfaces and the UTE is generally stable<sup>17</sup> so that neither social or ecological factors appear to influence the UTE, although this phase is not relevant to the present study, since the majority of Chinese cities had already entered the rapid development phase before 2000<sup>36</sup>. When a city enters a period of rapid development, natural surfaces are quickly replaced by impervious surfaces, and the UTE changes accordingly, as expressed here in the rapid increase phase. Social factors in this phase augment the UTE and a trade-off with ecological factors becomes apparent. Subsequently, the rate of urban may stabilize, and social factors may exert an influence through ecological protection policies such that the rate of UTE increase tends to decline (i.e., the slow increase phase). After entering the advanced

development period, achieving a livable city requires maintaining stable socio-economic growth while increasing eco-environmental protection, so UTE tends to decline (i.e., the decrease phase). Ecological factors limit or suppress the UTE at this stage but there is now synergy with social factors. This is illustrated well by the three largest urban agglomerations in China which all exhibit heat mitigation inflection points. Meanwhile, the UTE of Beijing also shows decreasing trend ( $SESI = 0.596$ ) (Supplementary Table 2). The capital city of China has ongoing population and economic growth and yet, despite this, exhibits an increasing trend in vegetation quality ( $slope_{\Delta EVI} = 0.003$ ). These suggest that urban development accompanied by socioeconomic growth are not necessarily detrimental to ecological protection and that win-win solutions for both society and ecology are feasible.

Our findings have important implications for the future development of more integrated strategies for urban heat mitigation. Parsing the SES structure layer by layer reveals the relative degree of influence of the various factors, pathways, and systems on UTE trends and offers several important insights for urban sustainability. In particular, we confirm the mitigating effect of ecological land area on the UTE as noted elsewhere<sup>17,37</sup>, a situation that may be enhanced by vertical greenery that has been shown reduce the exterior surface temperature by as much as 13 °C<sup>38</sup>. These results are mutually validated with our results. Moreover, unlike the results of some previous spatial analyses<sup>6,19</sup>, our results show that population density alone does not influence UTE. A previous study, presenting a 15-year time series analysis of 31 Chinese cities, also concluded that high population growth rates are not necessarily associated with high UTE<sup>14</sup>. It is predictable that the increase in population directly affects anthropogenic heat through metabolic growth, which generates much lower heat emissions than those generated by the other three anthropogenic heat sources, namely industry, transportation and buildings<sup>39</sup>. The indirect effect of population density on the UTE is reflected in its interaction with other factors, while the nonlinearly enhanced mode further highlights the importance of population density and, indeed, the impact of critical paths comprising both social and ecological factors also imply the need for an integrated, holistic strategy in relation to urban heat. A local scale study of a part of Rome, Italy, provides an example of how considering the issue more holistically through combining urban greening with adjustments to roof and pavement albedo may significantly reduce urban heat stress<sup>40</sup>. Such solutions recognize both pressures on, and resilience of the SES, as indicated by the SES status. While social factors such as population growth and construction land expansion may generally thought of as promoters of urban heat stress, the example of Beijing suggests that socioeconomic growth and ecological enhancement are not necessarily mutually exclusive, and that sustainable urban development can be achieved. Simultaneous socioeconomic development and ecological protection further enhances human well-being, creating a virtuous cycle. Accordingly, holistic solutions derived from the SES perspective are not only effective in mitigating the UTE, but also in addressing other urban challenges, such as biodiversity conservation, and flood and drought management<sup>41,42</sup>.

It should be noted that there remain constraints to this framework due to data limitations in terms of both social and ecological factors, whereby there are few relevant large-scale, long-time series datasets to guide specific actions. The SES, as considered here, may be more complex and have even more diverse pathways<sup>23</sup>. Although this study selects five representative factors, it is difficult to comprehensively characterize the impacts of SESs on the UTE. For example, the three anthropogenic heat sources, industry, transportation, and buildings, are not considered in the quantification of anthropogenic heat, which may result in an overestimation or underestimation of SESI. Furthermore, the inadequate accuracy for remote sensing datasets also introduces

errors in the quantification of UTE and SESI. For instance, the overall accuracy of the land cover dataset used in this study is 79.31%, and although the accuracy outperforms other same type products, much potential for improvement remains. In order to achieve more robust and reliable integrated heat mitigation strategies in the future, it is necessary to develop more dimensions, higher precision, large-scale datasets, and explore a broader range of both social and ecological factors and their interactions. The ultimate objective must surely be to achieve the most desirable SES state that optimizes the UTE for sustainable urban development.

In summary, this study aims to reveal the relationship between urban thermal environment (UTE) evolution and social-ecological system (SES) dynamics. Through the revealing of nonlinear growth patterns in the UTE over the last two decades in a substantial proportion of urban areas in China and its relationship to urban development, UTE evolution is further confirmed to conform to the Environmental Kuznets Curve. More importantly, this study highlights the impact of social and ecological system interactions and demonstrates that integrated strategies are prerequisites for urban heat mitigation. In particular, we emphasize the feasibility of win-win trajectories for both social and ecological systems in the face of multiple urban sustainability challenges.

## METHODS

### Study area

China is the largest country in eastern Asia and, in extending from 73.66°–135.05°E and 3.86°–53.55°N, it spans several climate zones (Supplementary Fig. 5). Chinese cities have undergone very rapid urbanization in the last few decades<sup>36</sup>, inevitably associated with a number of eco-environmental problems. More recently, the “New type Urbanization” and “Ecological Civilization Construction” in China have emerged with a focus on the harmonious development of both humans and nature. With its range of climate contexts and patterns of urbanization, China is an ideal study area to explore spatial-temporal trends in the evolving UTE. According to China’s seventh census in 2020, there are 101 prefecture-level cities with urban areas of more than one million people. However, during urban development, a city may form a polycentric pattern (i.e., two or more urban patches larger than 100 km<sup>2</sup> within the administrative boundary)<sup>43</sup> and the urbanization process even within the same city may differ. As a consequence, we recognized these as multiple samples and, accordingly identified a total of 136 urban areas as samples for this study.

### Remote sensing datasets

We used two datasets from the MODIS-terra satellite for the period 2000–2021, including the MOD11A2 land surface temperature product with an eight-day composite at a spatial resolution of 1 km, and the MOD13A2 enhanced vegetation index (EVI) product with a 16-day composite at a spatial resolution of 1 km. These MODIS datasets were obtained from National Aeronautics and Space Administration.

The nighttime lighting dataset at 1 km resolution for 2000–2021 was developed by integrating DMSP-OLS and SNPP-VIIRS data to obtain the improved DMSP-OLS data<sup>44</sup>.

The population density dataset was obtained from the WorldPop website, generated from census counts and a series of geospatial covariate projections.

The land cover type datasets were derived from Landsat TM images at 30 m resolution for 2000–2021 obtained from the China Land Cover Dataset<sup>45</sup>. Land cover was classified into nine categories, viz. cropland, forest, shrub, grassland, water, snow/ice, barren, impervious and wetland. This dataset had an overall accuracy of 79.31%, which outperformed other time-series land cover datasets and has been widely used<sup>45,46</sup>.



The urban area boundary data in 2018 was generated from a 30 m resolution artificial impervious area product. After multiple comparisons, the data have been shown to depict urban areas well, and the product has been widely used<sup>47,48</sup>. This study preprocessed the data through, firstly, extracting urban patches with an area >100 km<sup>2</sup>. The urban area boundaries within each city were then obtained by clipping the administrative boundaries of the city (The administrative boundary data used in this study, including national, provincial, and municipal levels, were obtained from the Resource and Environment Science and Data Centre of the Chinese Academy of Science). Finally urban areas were resampled to 1 km resolution and gaps within the urban area boundaries were filled.

### Urban thermal environment

We used land surface temperature to assess the intensity of the UTE. Note: This study is focused on finding solutions for mitigating UTE from a SES perspective applicable to various climate contexts, but SES management is difficult to do based on climate factors alone. Therefore, we used reference areas in the quantification of UTE to avoid disturbances caused by varying climatic backgrounds. The intensity of the UTE ( $\Delta T$ ) is quantified as the difference in land surface temperature between urban area ( $T_u$ ) and reference area ( $T_r$ ) in the same year, i.e.,  $\Delta T = T_u - T_r$ . Using the 2018 urban area boundary and reference area boundary to calculate  $\Delta T$  for 2000–2021. The reference area was determined by land cover type and EVI data and to meet the following requirements: (1) The reference area lies between 10–30 km buffers around the urban area. This buffer avoids interference from urban areas that are too adjacent to each other, while avoiding uncertainty regarding the climate context. Furthermore, buffering at this scale avoids the effects of small-scale land type changes. (2) Cropland or forest land within the buffers and with EVI > 0.4 was selected as the reference area, ensuring that land types in the reference area remain largely consistent across the study period. Note that altitude effects were not taken into consideration in the selection of reference areas since, although elevation influences the UTE intensity in mountainous cities, it does not influence the estimation of the interannual trend of UTE in each city<sup>14,15</sup>. Summer daytime is the time of the year when temperatures are highest, and heat stress is strongest for the urban population and vegetation<sup>49,50</sup>. Therefore, considering the aim to mitigate UTE of this study, we calculated  $\Delta T$  during the daytime in the summer (June - August) from 2000 to 2021, year by year.

To explore trends in the UTE in each urban area, we applied ordinary least squares linear regression and piecewise linear regression, with  $\Delta T$  as the dependent variable and year as the independent variable. Firstly, ordinary least squares linear regression was used to analyze the general trend of  $\Delta T$  in 136 urban areas over the period 2000–2021. The regression coefficient was used to measure the annual trend of  $\Delta T$ , and tested the model adjusted  $R^2$  and significance (two-tailed  $t$  test,  $p < 0.05$ ). This was followed by piecewise linear regression to detect the existence of inflection points in  $\Delta T$  over the last 22 years, and thereby identify phases in the evolving UTE. If no inflection point is observed, it implies that the UTE trend has remained unchanged and is in a steady state. The presence of an inflection point indicates that the UTE exhibits distinct trends before and after the inflection, suggesting the existence of two separate steady states. Piecewise linear regression can be expressed as

$$Y = \begin{cases} a_1X + b_1, X \leq T \\ a_2X + b_2, X > T \end{cases} \quad (1)$$

where  $Y$  is  $\Delta T$ ,  $X$  is year,  $T$  is the inflection point,  $a_1$  and  $a_2$  are the slopes of the linear segments before and after the inflection point, respectively,  $b_1$  and  $b_2$  are the intercepts of the linear segments before and after the inflection point, respectively.

Inflection points were selected using the following criteria: (1) The adjusted  $R^2$  of piecewise linear regression exceeds 0.6 as well as greater than the adjusted  $R^2$  of ordinary least squares linear regression. (2) The number of inflection points is limited to two or less, as it seems unlikely that more than three phases of thermal evolution would occur in 22 years. (3) Inflection points are restricted to the period 2003–2019 (i.e., not in the first or last three years) of the study time series, because it takes at least three years to reflect a change in the trend. (4) A significant difference in the slope of the two linear segments is observed before and after the inflection point (two-tailed  $t$ -test,  $p < 0.05$ ).

### Social and ecological factors

To reflect the complexity of urban SESs, we selected available and representative social and ecological factors from those most commonly used in the literature. In cities, blue and green spaces are important ecological factors and nature-based solutions to mitigate UTE. They regulate surface energy exchange processes through strong evapotranspiration and high albedo<sup>37</sup>. Hence, we chose two ecological factors, ecological land percentage and EVI, to represent the quantitative and qualitative characteristics of the ecosystem, respectively. For ecological land percentage, we calculated the percentage of the sum of cropland, forest, shrub, grassland, water and wetland in each urban area, year by year. For the EVI, the growth condition of vegetation is influenced by climate<sup>51</sup> so we observed the change in ecosystem quality by calculating the difference in EVI ( $\Delta EVI$ ) between the urban area ( $EVI_u$ ) and the reference area ( $EVI_r$ ), i.e.,  $\Delta EVI = EVI_u - EVI_r$ .

Two main processes were employed for estimating the direct impact of social systems on the UTE: increased anthropogenic heat from human activities, and enhanced surface heat storage from artificial impervious surfaces<sup>52</sup>. We chose three social factors, population density, nighttime light, and impervious area percentage to represent demographic<sup>17</sup>, economic development<sup>11</sup> and urban expansion<sup>20</sup>, respectively. Since the population density dataset is only updated to 2020, we used the 2020 data to represent 2021. Nighttime light data have an oversaturation phenomenon that masks the intensity differences within the saturated region<sup>53</sup>. Therefore, we corrected the nighttime light data based on the EVI data of the corresponding year<sup>53</sup>. The Vegetation Adjusted Nighttime Light Index ( $NL_{VA}$ ) ranges from 0 to 1, and provides a more detailed characterization of urban economic development than nighttime light. Impervious area percentage was calculated as the percentage of impervious area in the urban area based on year-by-year land cover type data.

Geographic detector models were used to quantify the effects of social factors, ecological factors, and social and ecological factor interactions on  $\Delta T$  trends. Geographic detector is a statistical method used to detect spatially stratified heterogeneity in geographical phenomena so as to reveal its underlying mechanisms<sup>54</sup>. Compared to statistical methods such as multiple linear regression, principal component analysis and random forest, geographic detectors have three advantages, viz. (1) enables nonlinear relationships between geographic phenomena and their driving factors to be identified; (2) collinearity between the driving factors has no effect on the results; (3) the contribution of the interaction of two driving factors to geographical phenomena can be detected. In this study, the factor detector module was used to analyze the role of individual social or ecological factors on  $\Delta T$  trends. Moreover, feedback paths formed by the interaction between social and ecological factors mean that social and ecological subsystems are intimately connected (Fig. 1), and thus the interaction detector module was used to explore the combined role of social and ecological factors on  $\Delta T$  trends. The degree of importance of each role is measured through the computation of a  $q$ -statistic, which has a range 0–1.

## Social-ecological system status

It is important to understand the state of a SES for socio-economic development as well as natural resource and disaster management<sup>55</sup>. In this study we constructed a social-ecological status index oriented to the UTE to reflect the structure and developmental status of the SES based on the concepts of resilience and pressure (Supplementary Fig. 6). Resilience is defined as the ability of a system to absorb and reduce possible heat stresses and to maintain, reorganize and develop its function. Pressure refers to the system's internal pressure and the UTE as a stressor, is defined as the positive effect of changes in system components on the  $\Delta T$ . In this study, social ( $S_i$ ) and ecological ( $E_i$ ) factors that exhibit positive correlations with the  $\Delta T$  are identified as pressure indicators, while negatively correlated factors are identified as resilience indicators (Supplementary Fig. 6a). Multiple feedback paths formed by the interaction between social and ecological factors jointly construct the SESI (Eq. (2)).

In computing the SESI, all indicators were first normalized to the range of 0–1 to avoid different dimensions and units among multiple factors. Secondly, each feedback path was calculated according to the difference between resilience indicator and pressure indicator, i.e.,  $R_i - P_i$ . The weight  $Q$  of each feedback path was determined based on the contribution of the interaction of social and ecological factors within that path to  $\Delta T$  trends (Supplementary Fig. 6b), i.e., the value of the  $q$ -statistic in the interaction detector module. Ultimately, the value of the SESI aimed at UTE ranges from  $-1$  (least desirable) to  $+1$  (most desirable). SESI was used to reveal the role of the SES on UTE (Supplementary Fig. 6c).

$$SESI = \sum_{i=1}^n Q_i (R_i - P_i) \quad (2)$$

where  $SESI$  is the social-ecological status index oriented at UTE,  $i$  is the feedback path,  $n$  is the number of the feedback paths,  $Q_i$  is the weight of the  $i$ -th feedback path,  $R_i$  and  $P_i$  are the resilience and pressure indicator of the  $i$ -th feedback path, respectively.

## Reporting summary

Further information on research design is available in the Nature Research Reporting Summary linked to this article.

## DATA AVAILABILITY

The MODIS data are publicly available at <https://adsweb.modaps.eosdis.nasa.gov>; the land cover type datasets is publicly available at <https://doi.org/10.5281/zenodo.4417810>; the nighttime lighting dataset is publicly available at <https://dataverse.harvard.edu/dataset.xhtml?persistentId=doi:10.7910/DVN/GYJGU>; the urban area boundary dataset is publicly available at <http://data.ess.tsinghua.edu.cn/>; the population dataset is publicly available at <https://www.worldpop.org>. The administrative boundary data is publicly available at <https://www.resdc.cn/>. All relevant data are available from the corresponding author upon reasonable request.

## CODE AVAILABILITY

All code used to produce the necessary data and results in this study are available in the following repository: <https://zenodo.org/record/8112168>.

Received: 12 July 2023; Accepted: 9 January 2024;

Published online: 22 January 2024

## REFERENCES

- Voogt, J. A. & Oke, T. R. Thermal remote sensing of urban climates. *Remote Sens. Environ.* **86**, 370–384 (2003).
- Liu, Z. et al. Surface warming in global cities is substantially more rapid than in rural background areas. *Commun. Earth Environ.* **3**, 219 (2022).
- Meehl, G. A. & Tebaldi, C. More intense, more frequent, and longer lasting heat waves in the 21st century. *Science* **305**, 994–997 (2004).
- Estoque, R. C. et al. Heat health risk assessment in Philippine cities using remotely sensed data and social-ecological indicators. *Nat. Commun.* **11**, 1581 (2020).
- Santamouris, M. Recent progress on urban overheating and heat island research. Integrated assessment of the energy, environmental, vulnerability and health impact. Synergies with the global climate change. *Energy Build* **207**, 109482 (2020).
- Manoli, G. et al. Magnitude of urban heat islands largely explained by climate and population. *Nature* **573**, 55–60 (2019).
- Li, D. et al. Urban heat island: aerodynamics or imperviousness? *Sci. Adv.* **5**, eaau4299 (2019).
- Mooney, H. A., Duraiappah, A. & Larigauderie, A. Evolution of natural and social science interactions in global change research programs. *Proc. Natl. Acad. Sci.* **110**, 3665–3672 (2013).
- Liu, J. et al. Provencher, coupled human and natural systems. *AMBIO: J. Hum. Environ.* **36**, 639–649 (2007).
- Clinton, N. & Gong, P. MODIS detected surface urban heat islands and sinks: global locations and controls. *Remote Sens. Environ.* **134**, 294–304 (2013).
- Peng, S. et al. Surface urban heat island across 419 global big cities. *Environ. Sci. Technol.* **46**, 696–703 (2012).
- Zhou, D., Zhao, S., Liu, S., Zhang, L. & Zhu, C. Surface urban heat island in China's 32 major cities: Spatial patterns and drivers. *Remote Sens. Environ.* **152**, 51–61 (2014).
- Zhou, D. et al. Satellite remote sensing of surface urban heat islands: progress, challenges, and perspectives. *Remote Sens.* **11**, 48 (2018).
- Yao, R. et al. Interannual variations in surface urban heat island intensity and associated drivers in China. *J. Environ. Manage.* **222**, 86–94 (2018).
- Yao, R., Wang, L., Huang, X., Gong, W. & Xia, X. Greening in rural areas increases the surface urban heat island intensity. *Geophys. Res. Lett.* **46**, 2204–2212 (2019).
- Chakraborty, T. & Lee, X. A simplified urban-extent algorithm to characterize surface urban heat islands on a global scale and examine vegetation control on their spatiotemporal variability. *Int. J. Appl. Earth Obs. Geoinf.* **74**, 269–280 (2019).
- Feng, R., Wang, F., Wang, K., Wang, H. & Li, L. Urban ecological land and natural-anthropogenic environment interactively drive surface urban heat island: an urban agglomeration-level study in China. *Environ. Int.* **157**, 106857 (2021).
- Dinda, S. Environmental kuznets curve hypothesis: a survey. *Ecol. Econ.* **49**, 431–455 (2004).
- Yuan, Y. et al. Natural-anthropogenic environment interactively causes the surface urban heat island intensity variations in global climate zones. *Environ. Int.* **170**, 107574 (2022).
- Zhou, D. et al. Spatiotemporal trends of urban heat island effect along the urban development intensity gradient in China. *Sci. Total Environ.* **544**, 617–626 (2016).
- Reyers, B., Folke, C., Moore, M.-L., Biggs, R. & Galaz, V. Social-ecological systems insights for navigating the dynamics of the anthropocene. *Annu. Rev. Env. Resour.* **43**, 267–289 (2018).
- Liu, J. et al. Complexity of coupled human and natural systems. *Science* **317**, 1513–1516 (2007).
- Alberti, M. et al. The complexity of urban eco-evolutionary dynamics. *BioScience* **70**, 772–793 (2020).
- Peng, J. et al. Spatiotemporal evolution of urban agglomerations in China during 2000–2012: a nighttime light approach. *Landsc. Ecol.* **35**, 421–434 (2020).
- Yang, L. & Li, Y. Low-carbon city in China. *Sustain. Cities Soc.* **9**, 62–66 (2013).
- He, B. et al. Co-benefits approach: opportunities for implementing sponge city and urban heat island mitigation. *Land Use Policy* **86**, 147–157 (2019).
- Kolokotsa, D., Lilli, A., Lilli, M. & Nikolaidis, N. On the impact of nature-based solutions on citizens' health & well being. *Energy Build* **229**, 110527 (2020).
- Kabisch, N. et al. Nature-based solutions to climate change mitigation and adaptation in urban areas: perspectives on indicators, knowledge gaps, barriers, and opportunities for action. *Ecol. Soc.* **21**, 39 (2016).
- Lafortezza, R. & Sanesi, G. Nature-based solutions: settling the issue of sustainable urbanization. *Environ. Res.* **172**, 394–398 (2019).
- Peng, J., Cheng, X., Hu, Y. & Corcoran, J. A landscape connectivity approach to mitigating the urban heat island effect. *Landsc. Ecol.* **37**, 1707–1719 (2022).
- Schwaab, J. et al. The role of urban trees in reducing land surface temperatures in European cities. *Nat. Commun.* **12**, 6763 (2021).
- Li, Y., Schubert, S., Kropp, J. & Rybski, D. On the influence of density and morphology on the Urban Heat Island intensity. *Nat. Commun.* **11**, 2647 (2020).
- Middel, A., Häb, K., Brazel, A., Martin, C. & Guhathakurta, S. Impact of urban form and design on mid-afternoon microclimate in Phoenix Local Climate Zones. *Landsc. Urban Plan.* **122**, 16–28 (2014).
- Schneider, F., Ortiz, J., Vanos, J., Sailor, D. & Middel, A. Evidence-based guidance on reflective pavement for urban heat mitigation in Arizona. *Nat. Commun.* **14**, 1467 (2023).
- Georgescu, M., Morefield, P., Bierwagen, B. & Weaver, C. Urban adaptation can roll back warming of emerging megapolitan regions. *Proc. Natl. Acad. Sci.* **111**, 2909–2914 (2014).
- Chen, M., Liu, W. & Tao, X. Evolution and assessment on China's urbanization 1960–2010: Under-urbanization or over-urbanization? *Habitat Int* **38**, 25–33 (2013).

37. Yu, Z. et al. Vejre, critical review on the cooling effect of urban blue-green space: a threshold-size perspective. *Urban Green* **49**, 126630 (2020).
38. Susorova, I., Angulo, M., Bahrami, P. & Brent, S. A model of vegetated exterior facades for evaluation of wall thermal performance. *Build. Environ.* **67**, 1–13 (2013).
39. Sailor, D. A review of methods for estimating anthropogenic heat and moisture emissions in the urban environment. *Int. J. Climatol.* **31**, 189–199 (2011).
40. Salata, F. et al. Relating microclimate, human thermal comfort and health during heat waves: An analysis of heat island mitigation strategies through a case study in an urban outdoor environment. *Sustain. Cities Soc.* **30**, 79–96 (2017).
41. Ding, M. & Wei, Y. A conceptual framework for quantitatively understanding the impacts of floods/droughts and their management on the catchment's social-ecological system (C-SES). *Sci. Total Environ.* **828**, 154041 (2022).
42. Martín-López, B. & Montes, C. Restoring the human capacity for conserving biodiversity: a social-ecological approach. *Sustain. Sci.* **10**, 699–706 (2015).
43. Lv, Y., Zhou, L., Yao, G. & Zheng, X. Detecting the true urban polycentric pattern of Chinese cities in morphological dimensions: a multiscale analysis based on geospatial big data. *Cities* **116**, 103298 (2021).
44. Wu, Y., Shi, K., Chen, Z., Liu, S. & Chang, Z. Developing improved time-series DMSP-OLS-like data (1992–2019) in China by integrating DMSP-OLS and SNPP-VIIRS. *IEEE Trans. Geosci. Remote Sens.* **60**, 1–14 (2022).
45. Yang, J. & Huang, X. The 30 m annual land cover dataset and its dynamics in China from 1990 to 2019. *Earth Syst. Sci. Data* **13**, 3907–3925 (2021).
46. Chen, S., Bao, Z., Ou, Y. & Chen, K. The synergistic effects of air pollution and urban heat island on public health: A gender-oriented nationwide study of China. *Urban Clim.* **51**, 101671 (2023).
47. Zhang, L. et al. Direct and indirect impacts of urbanization on vegetation growth across the world's cities. *Sci. Adv.* **8**, eabo0095 (2022).
48. Chen, B. et al. Contrasting inequality in human exposure to greenspace between cities of Global North and Global South. *Nat. Commun.* **13**, 4636 (2022).
49. Wei, X. et al. Analysis of vegetation vulnerability dynamics and driving forces to multiple drought stresses in a changing environment. *Remote Sens.* (2022) <https://doi.org/10.3390/rs14174231>.
50. Chen, B. et al. Heat risk of residents in different types of communities from urban heat-exposed areas. *Sci. Total Environ.* **768**, 145052 (2021).
51. Wu, D. et al. Time-lag effects of global vegetation responses to climate change. *Glob. Chang. Biol.* **21**, 3520–3531 (2015).
52. Wang, J. et al. Anthropogenic emissions and urbanization increase risk of compound hot extremes in cities. *Nat. Clim. Chang.* **11**, 1084–1089 (2021).
53. Lu, D., Tian, H., Zhou, G. & Ge, H. Regional mapping of human settlements in southeastern China with multisensor remotely sensed data. *Remote Sens. Environ.* **112**, 3668–3679 (2008).
54. Song, Y., Wang, J., Ge, Y. & Xu, C. An optimal parameters-based geographical detector model enhances geographic characteristics of explanatory variables for spatial heterogeneity analysis: cases with different types of spatial data. *GISci. Remote Sens.* **57**, 593–610 (2020).
55. Estoque, R. & Murayama, Y. Social-ecological status index: a preliminary study of its structural composition and application. *Ecol. Indic.* **43**, 183–194 (2014).

## ACKNOWLEDGEMENTS

This study is supported by the National Key R&D Program of China (No. 2022YFE1303102) and the Global Engagement for Strategic Partnership project of Nanjing University.

## AUTHOR CONTRIBUTIONS

B.C. and F.K., designed the research. B.C., F.K. and M.M., wrote the paper. B.C. and H.P., conducted data analysis and calculation. F.K., M.M., A.Z., L.C. and L.Y., contributed to the interpretation and review of the results. All authors approved the manuscript for submission.

## COMPETING INTERESTS

The authors declare no competing interests.

## ADDITIONAL INFORMATION

**Supplementary information** The online version contains supplementary material available at <https://doi.org/10.1038/s42949-024-00141-4>.

**Correspondence** and requests for materials should be addressed to Fanhua Kong or Michael E. Meadows.

**Reprints and permission information** is available at <http://www.nature.com/reprints>

**Publisher's note** Springer Nature remains neutral with regard to jurisdictional claims in published maps and institutional affiliations.



**Open Access** This article is licensed under a Creative Commons Attribution 4.0 International License, which permits use, sharing, adaptation, distribution and reproduction in any medium or format, as long as you give appropriate credit to the original author(s) and the source, provide a link to the Creative Commons license, and indicate if changes were made. The images or other third party material in this article are included in the article's Creative Commons license, unless indicated otherwise in a credit line to the material. If material is not included in the article's Creative Commons license and your intended use is not permitted by statutory regulation or exceeds the permitted use, you will need to obtain permission directly from the copyright holder. To view a copy of this license, visit <http://creativecommons.org/licenses/by/4.0/>.

© The Author(s) 2024